# Elastic scattering and transfer in the $^6$He + $^{209}$Bi system below the Coulomb barrier.

E.F. Aguilera[1], J.J. Kolata[2], F.D. Becchetti[3], P.A. DeYoung[4], J.D. Hinnefeld[5], Á. Horváth[6], L.O. Lamm[2], Hye-Young Lee[2], D. Lizcano[1], E. Martinez-Quiroz[1], T.W. O'Donnell[3], D.A. Roberts[3], and G. Rogachev[2].

[1] *Departamento del Acelerador, Instituto Nacional de Investigaciones Nucleares, A.P. 18-1027, C.P. 11801, Mexico, D.F.*

[2] *Physics Department, University of Notre Dame, Notre Dame, Indiana 46556-5670*

[3] *Physics Department, University of Michigan, Ann Arbor, Michigan 48109-1120*

[4] *Physics Department, Hope College, Holland, MI 49422-9000*

[5] *Physics Department, Indiana University South Bend, South Bend, Indiana 46634-7111*

[6] *Department of Atomic Physics, Eötvös Loránd University, Pázmány P. sétány 1/A, H-1117 Budapest, Hungary and Cyclotron Laboratory, Michigan State University, East Lansing, Michigan 48824-1321*

(January 26, 2001)

The interaction of $^6$He with $^{209}$Bi has been studied over a range of energies well below the nominal Coulomb barrier. A $^4$He group of remarkable intensity, first observed in a previous experiment at near-barrier energies, continues to dominate the reaction in the sub-barrier regime. A total cross section of nearly 200 mb was measured for this group at 5 MeV below the barrier. This very large value is shown to be consistent with the total reaction cross section deduced from a simultaneously-measured elastic scattering angular distribution.

PACS Numbers: 25.60.-t, 25.60.Gc, 25.60.Je, 27.20.+n

In a recent Letter [1], we reported the discovery of an exceptionally strong $^4$He group resulting from transfer and/or breakup modes in the interaction of the exotic "Borromean" [2] nucleus $^6$He with a $^{209}$Bi target. The integrated cross section of this group far exceeds the total fusion yield [3] in the region of the barrier. The sum of the fusion plus "breakup/transfer" yield saturates the total reaction cross section predicted from an analysis of simultaneously-measured elastic scattering angular distributions. In view of the large magnitude of the $^4$He yield near the barrier, we have extended the measurement to energies that are well below the nominal barrier. In the present work, we report an excitation function for "breakup/transfer" down to a center-of-momentum (cm) energy of 14.3 MeV, which is approximately 5 MeV below the nominal Coulomb barrier of the $^6$He + $^{209}$Bi system. The results confirm the highly-anomalous nature of this process.

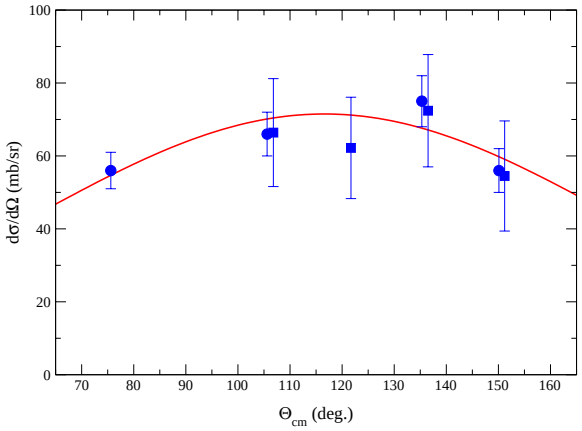


FIG. 1. Angular distribution at $E_{cm}$ = 18.6 MeV. The dotted points are taken from Ref. [1].

The experimental method has been discussed in Ref. [1]. The $^6$He beam was produced by the *TwinSol* radioactive nuclear beam (RNB) facility at the University of Notre Dame [4]. Two large superconducting solenoids act as thick lenses to collect and focus the secondary beam of interest onto a spot that is typically 5 mm full width at half maximum (FWHM). The primary beam was $^7$Li at an energy of 27.5 MeV, incident on a gas target with a 2 $\mu$m Havar entrance window. The cell was 2.5 cm long and contained He gas at a pressure of 1 atm to cool the exit window, a 12 $\mu$m foil of $^9$Be in which $^6$He is produced via the $^9$Be($^7$Li,$^6$He) proton transfer reaction. Primary beam currents of up to 300 particle·nA (pnA) were available, resulting in a maximum $^6$He rate of $10^5$ s$^{-1}$. The secondary beam flux was calibrated by inserting a Si ΔE-E telescope at the secondary target position and reducing the intensity of the primary beam by three orders of magnitude, so that the $^6$He particles could be directly counted while at the same time the primary beam current was measured in a Faraday cup. The secondary beam was contaminated by ions having the same magnetic rigidity as the desired $^6$He beam. This contamination was reduced by placing an 8 $\mu$m Havar foil at the crossover point between the two solenoids. Differential energy loss then helps to eliminate unwanted ions from the beam prior to the secondary target, which was a 3.2 mg/cm$^2$ Bi layer evaporated onto a 100 $\mu g/cm^2$ polyethylene backing and oriented so that its normal was at 12$^o$ to the beam. The remaining contaminant ions were identified by time-of-flight (TOF) techniques. The TOF of the particles was obtained from the time difference between

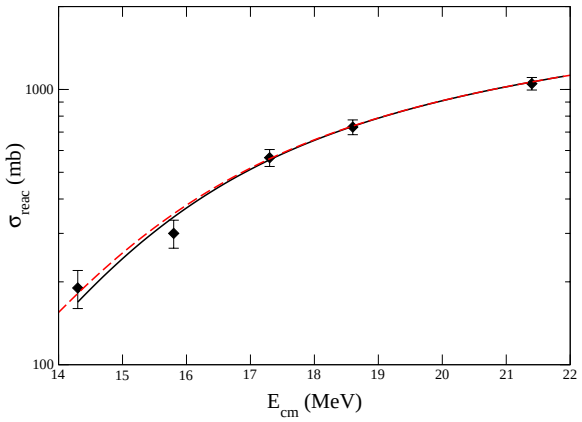


FIG. 2. Excitation function for the total reaction cross section. This is the sum of the angle-integrated $^4$He yield with the fusion cross section reported in Ref. [3]. See text for a discussion of the curves.

the occurrence of the secondary reaction and the RF timing pulse from a beam buncher. The time resolution of better than 3 ns (FWHM) was adequate to separate $^6$He from all contaminants, except for $^3$H which has the same mass-to-charge ratio and therefore the same velocity as $^6$He. However, it was shown in Ref. [1] that the $^3$H contaminant does not produce events in the energy region of interest for this experiment. The initial laboratory energy of the $^6$He beam was 19.4 MeV. This was reduced to lower values via energy loss in various combinations of 30 $\mu$m polypropylene and and 51 $\mu$m Mylar foils. In all cases, the energy resolution of the beam was approximately 1.5 MeV FWHM.

The reaction events were detected with five Si $\Delta$E-E telescopes placed at various angles on either side of the beam. Each telescope had a circular collimator that subtended a solid angle of 13 msr, corresponding to an effective angular resolution of 6$^o$ (FWHM), computed by folding in the acceptance of the collimator with the spot size and angular divergence of the beam. As in the previous work [1], we observed a strong, isolated group of $^4$He ions at a mean Q-value of about -2.5 MeV. The angular distributions obtained for this group (see Fig. 1 for an example) are broad, approximately Gaussian in form, and agree quite well with those reported in Ref. [1], where overlapping data exist. They are also similar in shape to those recently measured for $^6$Li+$^{208}$Pb near the barrier [5]. The total reaction cross sections, obtained by summing the angle-integrated $^4$He yield with the fusion cross section deduced from the data reported in Ref. [3], are shown in Fig. 2. The highest-energy point comes from the previous experiment; apart from this one, and the point at 18.6 MeV, fusion makes a negligible contribution to the total reaction cross section. For example, the fusion cross section at 17.3 MeV (obtained from an extrapolation of the data shown in Ref. [1]) is only 6% of the total cross section at this energy; the fractional contribution at lower energies is even smaller. Remarkably, the "transfer/breakup" yield is still nearly 200 mb at a cm energy of 14.3 MeV, which is about 5 MeV below the nominal barrier. In contrast, the $^6$Li+$^{208}$Pb cross section is already below 10 mb at a similar energy relative to the barrier [6].

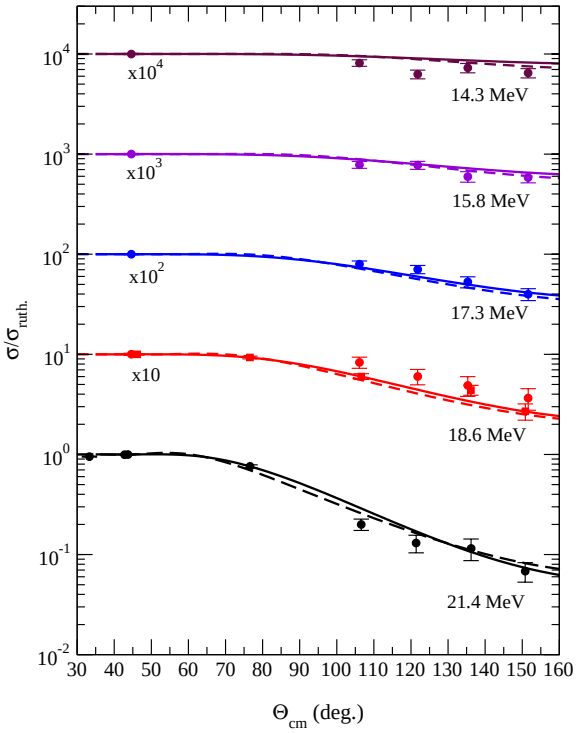


FIG. 3. Elastic scattering angular distributions for $^6$He+$^{209}$Bi. The cm energies corresponding to each distribution are given; the data at 21.4 MeV are taken from Ref. [1]. The solid curves were generated using a phenomenological optical-model potential with an energy- dependent imaginary diffuseness parameter. The dashed curves are calculations due to Mohr [9].

Simultaneously-measured elastic scattering angular distributions confirm the remarkable behavior of the total reaction cross section discussed above. These distributions are shown in Fig. 3. The 21.4-MeV angular distribution is taken from Ref. [1], and the 18.6-MeV point from this reference was repeated, as noted above. The solid curves in this figure are the result of optical-model fits to the data. The parameters of these fits are discussed in more detail below. The total reaction cross section predicted by the optical model is shown as the solid curve in Fig. 2. Thus, the same parameters that fit the elastic data also generate a reaction cross section in agreement with experiment. This is an important confirmation of the very large reaction cross sections that

have been measured since it suggests, for example, that the absolute normalization of the reaction data has been properly computed.

The optical-model parameters that have been used are purely phenomenological. It was found to be necessary and sufficient to vary only one parameter: the imaginary diffuseness. Equivalent fits can be generated by varying the imaginary radius parameter instead, but not the imaginary well depth unless an exceptionally strong variation in this parameter (far stronger than the variation reported by Signorini, *et al.* [7] in their study of $^{9}$Be+$^{209}$Bi elastic scattering) is deemed to be acceptable. The well-depth, radius, and diffuseness parameters of the real Woods-Saxon potential were 150 MeV, 7.95 fm, and 0.68 fm, respectively. The depth and radius of the volume Woods-Saxon imaginary potential were 25 MeV and 9.38 fm, respectively. Finally, the imaginary diffuseness was given by:

$$a_I = (1.964 - 0.045E_{cm}) \quad \text{fm}. \tag{1}$$

The predicted angular distributions are not very sensitive to the parameters of the real potential, consistent with the observation that the $^{6}$He+$^{209}$Bi system is dominated by absorption from the elastic channel. Mohr [8] has used a folding model based on systematics of $\alpha$-nucleus potentials and found excellent agreement with the data of Ref. [1]. Fits to the present elastic-scattering data generated in this model [9] are shown as the dashed curves in Fig. 3. The depth of the imaginary potential, taken to be of Woods-Saxon form, was computed from the Brown-Rho formula [10] for the volume integral of the potential, with $J_0 = 127$ MeV fm$^3$ and $\Delta = 12.7$ MeV. The radius parameter was given by:

$$\mathrm{R_I} = (5.341 + 131.7/\mathrm{E_{cm}}) \quad \text{fm}. \tag{2}$$

All other parameters were the same as those given in Ref. [9]. In this approach, the anomalous behavior of the total reaction cross section is encapsulated in the very large imaginary radius parameter, rather than in the diffuseness parameter as above. It can be seen that the predictions of this model agree very well with those generated using an energy-dependent imaginary diffuseness parameter.

Another approach to parameterizing the energy dependence of the total reaction cross section is the model of Wong [11], in which the complex, energy-dependent optical model potential is replaced by an inverted harmonic oscillator potential. The reaction cross section is then computed from the barrier penetration probability, leading to the formula:

$$\sigma_{reac} = (\frac{\hbar\omega \mathrm{R}^2}{2\mathrm{E_{cm}}}) \ln(1 + \exp(\frac{2\pi}{\hbar\omega}[\mathrm{E_{cm}} - \mathrm{V_b}])) \tag{3}$$

Here, $V_b$ is the barrier height, $\hbar\omega$ is the oscillator parameter which determines the diffuseness of the potential, and R is the radius of the system at the barrier. The data in Fig. 2 can be fit with $V_b$=14.5 MeV, $\hbar\omega$=8.0 MeV, and R=10.75 fm, leading to an excitation function (dashed curve) which is almost indistinguishable from the optical-model fit using an energy-dependent imaginary diffuseness parameter, except at the lowest energy where it in fact yields a slightly better fit to the experiment. The barrier height is about 5 MeV less than the nominal Coulomb barrier for the $^{6}$He+$^{209}$Bi system, and the effective potential is also rather diffuse since it has an oscillator parameter that is about twice the typical value. However, the radius parameter is close to its expected value [12].

It is rather remarkable that the simple Wong model does such an excellent job of reproducing the observed energy dependence of the total reaction cross section. As discussed above, the optical model with complex Woods-Saxon potentials requires a strong energy dependence in the geometry of the imaginary well to give similar-quality fits to the data. This implies that the effective potential is not very well described by a Woods-Saxon form, which is perhaps not surprising. However, there appears to be no obvious explanation for the fact that barrier penetration through a real, quadratic, energy-independent potential describes the data as well as it does. It is also interesting to note that the 5 MeV reduction in the nominal barrier agrees very well with that needed to explain the fusion cross section [3]. This can be understood in the context of coupling between the breakup and fusion cross sections, as discussed in Refs. [13,14]. Another point concerns the relationship between the diffuse absorptive potential required to explain the experimental total reaction cross section and the so-called "threshold anomaly" in elastic scattering [15]. This anomaly manifests itself as a rapid energy dependence of the real nuclear potential near the barrier. Dispersion relations [15] predict an attractive "polarization" potential resulting from the normal, rapid reduction in absorption below the barrier. In the present situation, the absorption does not decrease rapidly below the barrier, and one therefore expects no anomaly. Absence of the anomaly for weakly-bound systems has been discussed by Mahaux, Ng$\hat{o}$, and Satchler [16], and appears to occur for the $^{6}$Li+$^{208}$Pb system [17], as well as for $^{6}$Li+$^{28}$Si [18]. In the present case, we can fit the elastic data with an energy-independent real potential, as expected in the absence of the anomaly. However, the absorption is so strong and of such long range that the sensitivity of the data to the real potential is not very great, which might obscure any sign of energy dependence even if it were present.

In summary, we have measured an excitation function for transfer/breakup in the $^{6}$He + $^{209}$Bi system below the Coulomb barrier. This process was shown in a recent experiment [1] to be exceptionally strong, accounting for over 80barrier. The corresponding $\alpha$-particle yield is a factor of four greater than that observed [5] for

$^6$Li + $^{208}$Pb at the barrier. In the present work, we show that transfer/breakup saturates essentially all the sub-barrier reaction cross section. The yield remains remarkably large, amounting to nearly 200 mb at 5 MeV below the barrier, which is a factor of 20 greater than that for $^6$Li+$^{208}$Pb at a similar energy relative to the barrier [6]. Extrapolation of the trend observed for $^6$He + $^{209}$Bi suggests that the $\alpha$-particle emission cross section will be in the range from 1-10 mb at a cm energy of 10 MeV, *i.e.*, one-half the nominal barrier height.

Simultaneously-measured elastic scattering angular distributions have been analyzed in the context of the optical model. The total reaction cross sections deduced from these data agree very well with the sum of the transfer/breakup and fusion yields. Energy- dependent absorptive potentials are required in order to reproduce the measured angular distributions. In particular, it was found that the geometry of the Woods-Saxon imaginary potential well varies as a function of energy, becoming more diffuse and extended at lower energies. An alternative approach, involving an increasing radius for the imaginary well at lower energies [9], appears to give equivalent results. The total reaction cross section near to and below the barrier can also be reproduced by a very simple barrier-penetration model due to Wong [11]. Although there are three adjustable parameters in this model, the entire excitation function is reproduced with a single choice of values. One of these parameters, the effective height of the barrier, is 5 MeV less than the nominal Coulomb barrier for $^6$He + $^{209}$Bi. This shift is completely consistent with that deduced from a previous measurement of the fusion cross section [3]. Another parameter, which measures the diffuseness of the effective potential, is very large compared with its typical value for normal nuclear systems. The third parameter, the interaction radius, is quite normal however.

The observed anomalous behavior of the fusion and breakup/transfer yields below the barrier is presumably related to the very weak binding of $^6$He, which may in turn lead to a large spatial extent for the radial wave function of the last two neutrons and an enhanced breakup cross section due to the fragile nature of the system. However, all of the analysis to date has been purely phenomenological. It would be very interesting to compare our data with detailed reaction calculations based on realistic models of $^6$He. Unfortunately, complete calculations of this kind are presently unavailable, though a qualitative study of the $^{11}$Be + $^{208}$Pb system [19] has recently appeared.

This work was supported by the National Science Foundation under Grant Nos. PHY99-01133, PHY98-04869, PHY00-72314, and PHY98-70262, and by the CONACYT (Mexico).

[1] E.F. Aguilera, *et al.*, Phys. Rev. Lett. **84**, 5058 (2000).
[2] M.V. Zhukov, *et al.*, Phys. Rep. **231**, 151 (1993).
[3] J.J. Kolata, *et al.*, Phys. Rev. Lett. **81**, 4580 (1998).
[4] M. Y. Lee, *et al.*, Nucl. Instrum. Methods in Phys. Research **A422**, 536 (1999).
[5] G.R. Kelly, *et al.*, Phys. Rev. C**63**, 024601 (2001).
[6] R. Ost, E. Speth, K,O, Pfeiffer, and K. Bethge, Phys. Rev. C**5**, 1835 (1972).
[7] C. Signorini, *et al.*, Phys. Rev. C**61**, 061603R (2000).
[8] P. Mohr, Phys. Rev. C**62**, 061601R (2000).
[9] P. Mohr, private communication.
[10] G.E. Brown and M. Rho, Nucl. Phys. **A372**, 397 (1981).
[11] C.Y. Wong, Phys. Rev. Lett. **31**, 766 (1973).
[12] L.C. Vaz, J.M. Alexander, and G.R Satchler, Phys. Rep. **69**, 373 (1981).
[13] C. Dasso and A. Vitturi, Phys. Rev. C**50**, R12 (1994).
[14] C. Dasso, *et al.*, Nucl. Phys. **A597**, 473 (1996).
[15] M.A. Nagarajan, C. Mahaux, and G.R. Satchler, Phys. Rev. Lett. **54**, 1136 (1985).
[16] C. Mahaux, C. Ngô, and G.R. Satchler, Nucl. Phys. **A449**, 354 (1986).
[17] N. Keeley, *et al.*, Nucl. Phys. **A571**, 326 (1994).
[18] M.A. Tiede, D.E. Trcka, and K.W. Kemper, Phys. Rev. C**44**, 1698 (1991).
[19] K. Hagino, A. Vitturi, C.H. Dasso, and S.M. Lenzi, Phys. Rev. C**61**, 037602 (2000).